The Fourth IEEE RAS/EMBS International Conference
on Biomedical Robotics and Biomechatronics
Roma, Italy. June 24-27, 2012

Design of a back-driveable actuation system for modular control of tendon-driven robot hands

Randall B. Hellman, *Student Member, IEEE* and Veronica J. Santos, *Member, IEEE*

Abstract— **This paper presents a novel design of a rotary motor-based actuation system for tendon-driven robotic hands. The system features a two-stage, zero backlash, pretensioned pulley reduction that enables high precision control of tendon displacement and force, as well as back-driveability of the motor. While the modular actuation system can be used to actuate any tendon-driven mechanism, the system is designed to meet or exceed the speed and strength of human fingertips. The actuation system is capable of operating up to 10 Hz before there is significant degradation of the system gain. The capabilities of the system are further demonstrated through the control of a Shadow Dexterous Robot Hand index finger at low (1 Hz) and high (4 Hz) frequencies. A single actuation unit can be duplicated for use in a single-acting actuation scheme ("2N-type") of N joints, but was designed specifically for a double-acting actuation scheme ("N-type") with "push-pull" capabilities. In the former case, one motor is used for each rotation direction of a single revolute joint. In the latter case, one motor can control both directions of the joint, thereby reducing hardware needs and control complexity. To address the challenges of tendon slack in the flexible-link transmission to the robot hand, the system includes a lead screw mechanism for setting a tension preload and springs for maintaining tension during the course of use. An integrated uniaxial load cell allows for monitoring of tendon tension and calculation of finger joint torques.**

I. Introduction

THE design of human-sized artificial hands is challenged by the relatively small volume available for sensor, actuator, and plant components. An intrinsic actuation approach (with motors in the fingers and palm) results in a compact and elegant form (e.g., [1]), but often at the expense of finger motion and force production capabilities. When both strength and speed are desired, an extrinsic actuation approach can be taken similar to that of the human hand. In addition to smaller intrinsic muscles in the palm, powerful extrinsic muscles in the forearm transmit torques to finger joints through tendons and extensor hoods that pass over the joints [2]. For practical reasons, many robot hands have actuators located proximal to the wrist and rely on cables to transmit torques about finger joints. Such tendon-driven designs have been used for underactuated [3] and robotic hands [4–8], prosthetic hands [9], and complex, anthropomorphic systems [10], [11].

Here we present a novel design for a rotary motor-based actuation system for a single revolute joint of a tendon-driven robotic hand. The actuation system was designed for a double-acting actuation scheme ("N-type") in which one motor can control both rotation directions of a single revolute joint [12]. This "push-pull" capability reduces hardware and control complexity. However, the modular actuation system could be duplicated and used in a single-acting actuation scheme ("2N-type") in which two motors actuate a single joint using an agonist/antagonist control scheme if co-contraction is desired. While the actuation system can be applied to any tendon-driven mechanism, the design criteria were created with a human-sized, anthropomorphic robot hand in mind. The actuation system is designed for use in a robotic hand testbed that allows for seamless transitions between different tendon-driven end effectors.

II. Methods

A. Design Criteria

Strength, speed, precision, and robustness are key features to consider in the design of remote actuation systems [13] for tendon-driven robotic hands. These features affect the ability of the fingertips to achieve the responsiveness necessary for implementation of artificial grip reflexes and the dexterity required for object manipulation during grasp. In particular, the use of flexible-link transmission systems (e.g., pulley- and sheath-routed tendons) adds to the design challenge [13].

The actuation system must have sufficient bandwidth and minimal phase delay so as to produce a fingertip force with minimal lag. Furthermore, proprioception capabilities are especially important. Motor encoders can provide tendon displacement and velocity measurements that, coupled with a known Jacobian matrix for the robot hand, could supplement joint angle and velocity data provided by the robot hand itself. In some cases, motor controllers can also provide motor current measurements as a method to determine joint torques. However, the desired method to determine joint torques will be through the use of uniaxial load cells in series with each tendon. In the actuation system

This work was supported in part by the NSF CPS Award 0932389.

R. B. Hellman is with the Department of Mechanical and Aerospace Engineering, Arizona State University, Tempe, AZ 85287 USA (e-mail: rhellman@asu.edu).

V. J. Santos is with the Department of Mechanical and Aerospace Engineering, Arizona State University, Tempe, AZ 85287 USA (e-mail: veronica.santos@asu.edu).

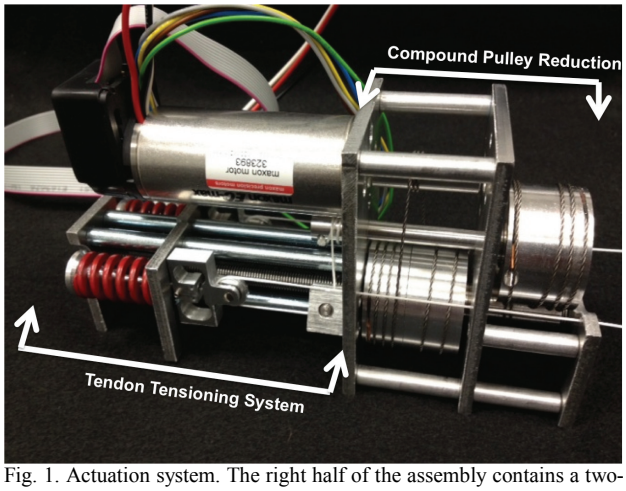

Fig. 1. Actuation system. The right half of the assembly contains a two-stage, zero backlash, 12:1 compound pulley reduction. Below the motor on the left are the tendon stiffness and preload mechanisms along with the inline load cells for measuring tendon tension.

presented here, the compound pulley reduction produces a desired high tendon force output along with zero backlash back-driveability (Fig. 1). The tendon preload and stiffness mechanisms, as well as the tendon tension sensors, are all located alongside a single Maxon EC-max 30 (30 mm diameter), 60 watt motor (Maxon Precision Motors, Inc.).

High factors of safety were used in the design of the actuation system in order to minimize performance limitations that might prohibit fast, reflex-like movements or functionally meaningful fingertip forces. Importantly, we are able to reduce the maximum motor current in order to accommodate different tendon-driven end effector designs without the actuation system itself limiting the performance of the overall robotic system. The motor bank is capable of achieving high forces that exceed the suggested maximum tendon tension of the Shadow Dexterous Robot Hand (Shadow Robot Company). To prevent damage to the end effector, a mechanical tendon fuse will be used as a secondary precaution in addition to software limitations on motor current. The mechanical fuse will be located serially in between the input tendons of the robotic hand and the output tendons of the actuation system. If the system were unexpectedly overloaded and the springs in the actuation system were unable to absorb the load, the mechanical fuse would fail, thereby sparing the robot hand from damage.

1) Compound pulley reduction

The motor module has a two-stage, 12:1 zero backlash compound pulley reduction from the motor shaft to the final output shaft (Fig. 2). Based on the 60 watt specifications, stall torque of the Maxon EC-max motor will sustain tendon tensions at the output shaft of 533N (120 lbf) with a nominal dynamic load of 58N (13 lbf) (Table 1). Although pulleys are mounted on ball bearing-supported shafts, the actual tendon forces will be slightly less due to frictional losses in the system. The fingertip force will vary depending on the actuation Jacobian that is unique to the design of the end effector that is in use.

Each stage of the independent pulley reduction consists of a double-wrapped wire rope (1/32" diameter, 3x7 hollow-core, McMaster-Carr #3458T51) that has both of its attachment points on the main pulley and is double-wrapped around the pinion. The double-wrap around the pinion ensures sufficient friction such that the wire rope will not slip over the pinion as it "walks" during pinion rotation. Inspired by tendon tensioning mechanisms in the Barrett WAM (Barrett Technology), tension in each independent loop of wire rope is maintained with a one-way bearing housed inside of a larger pulley, which maintains a desired preload in the wire rope (Fig. 2b). Crimped copper stop sleeves (McMaster-Carr #3897T31) at each end of the wire rope are held in place by grooves at wire rope attachment points on each half of the two-part pulley.

From the motor output shaft to the final output shaft, the system has zero backlash and is back-driveable. Zero

Table 1.

Actuation System Specifications	
Tendon Force	
Dynamic Operating Range	58 N (13 lbf)
Motor Stall Torque (Max Tendon Force)	533 N (120 lbf)
Tendon Displacement	5 cm
Tendon Tensioner Adjustment	14 cm
Module	
Dimensions	161 mm x 87 mm x 50 mm
Weight	834 g

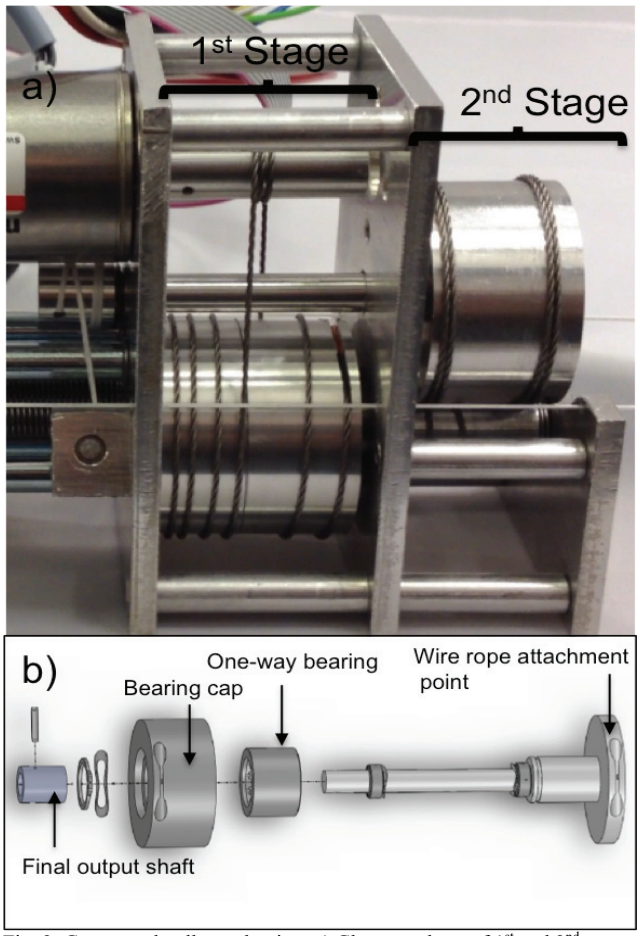

Fig. 2. Compound pulley reduction. a) Close up photo of 1st and 2nd stages of the compound pulley reduction. b) Exploded view of the "secondary pulley," in reference to the second reduction of the compound reduction).

backlash allows angular position/velocity and torque of the motor output shaft to be transformed according to the 12:1 reduction ratio with little loss at the final output shaft. Zero backlash also allows for back-driveable control of individual joints which simplifies the design of the actuation system as well as its modeling and control. The zero backlash pulley reduction and tensioning provided by a one-way bearing in each pulley serve to maintain a preload in the wire rope and prevent slack and unspooling. The relative rotation between each stage of the pulley reduction is kept fixed through the use of inextensible wire rope that is robust to creep. When first assembling, it takes a few cycles before the wire rope attains a stable position and rewraps in the same location. Once the desired wrap around the pulley is achieved, the rewrap position stays constant.

2) Tendon tensioning system

After the 12:1 compound pulley reduction, the final output shaft transitions to the tendons that actuate the robot hand. The tendon is comprised of a 0.7 mm diameter, monofilament fishing line (200 lbf Spectra line, Power Pro) line will be routed through low friction sheathing having an inner diameter of 1.2 mm and wall thickness of 0.3 mm. From the output shaft, the tendons are routed across two pulleys to enable the use of mechanisms for pre-tensioning the tendons, maintaining tendon tension and absorbing unexpected loads during use, and directly measuring tendon tension (Fig. 3). Due to the routing configuration of each tendon across a single pulley that attaches to a custom uniaxial load cell, the load cell measurements will be equal to twice the tendon tension. The load cell measurements can be used to monitor tendon tension directly and calculate finger joint torques.

Custom uniaxial load cells were designed specifically for the expected tendon force range of 0-530 N (0-120 lbf) with a resolution of 0.01 N (0.04 lbf). Each load cell has a full Wheatstone bridge with all strain gauges located on the interior of the load cell. The signal is amplified locally with an op-amp mounted to the load cell and a shield will cover all electrical components. Shielding on the load cell is required because the Maxon motor is in close proximity and will otherwise introduce significant noise into the load cell data. Each load cell serves as the main rigid link between the tendon and a die spring that maintains tendon stiffness.

The load cell is mounted on the opposite side of a guide plate and pinned to a die spring guide shaft that determines the tendon response to unanticipated loads and sets/maintains initial tendon preload and stiffness. The load cell itself is secured to an adjustable guide plate with two guide rails and a lead screw (Fig. 3b). Left-right adjustment of the guide plate (and spring-loaded tensioning mechanism) via rotation of the lead screw allows for changes in tendon lengths of up to 14 cm and tendon preload once tendon slack has been taken up. This tendon preload feature reduces overall setup time when an end effector is newly attached and simplifies adjustments that may be necessary due to the development of slack in tendons within the robot hand. Tendon tension will be incorporated into the control structure for determining finger joint torques and as a safety feature to prevent joint failure or system damage.

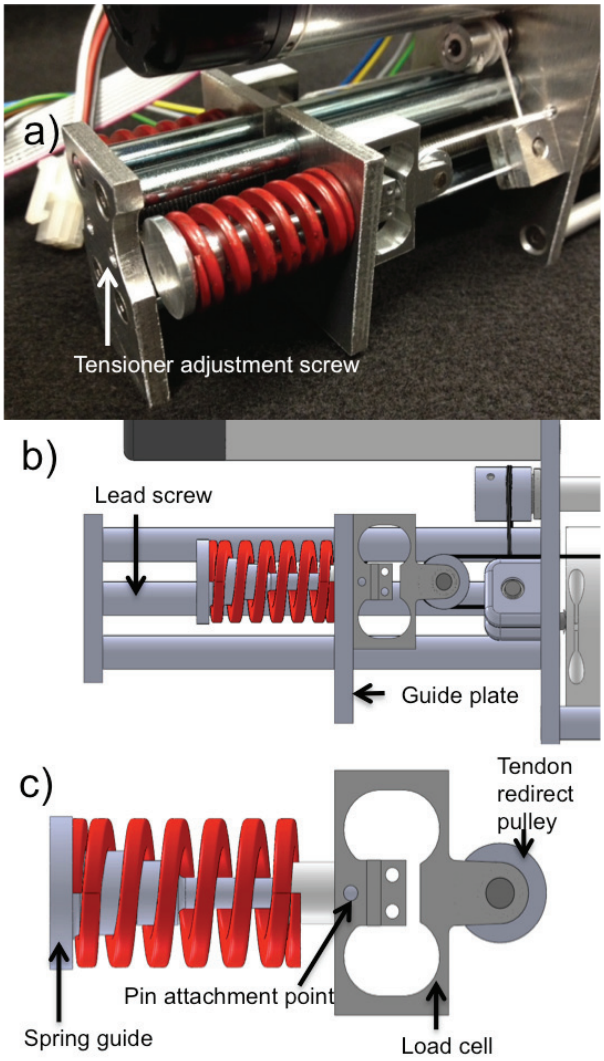

Fig. 3. Tendon tensioner, stiffness, and load cell. Tendon stiffness is determined by the modular spring (shown in red). Tendon preload and tension is adjusted by moving the guide plate along the lead screw with the tension adjustment screw (a-b). A custom uniaxial load cell is attached to the spring guide with a 1/16" diameter spring pin that constrains the assembly c) to the guide plate (a-b) for direct measurement of tendon tension.

An early design of the tendon tensioning assembly included a simple mechanism for achieving non-linear stiffness (as in [14]) where the tendon passed over a spring and, as the spring compressed, the angle of action over the spring changed. For compactness of design and to keep the spring tensioning and tendon routing in a single plane (reducing hardware needs for redirecting tendons) we created the design presented here. The die spring in the modular tendon tensioning assembly can be changed to suit the tendon stiffness requirements of the user. This will affect the end effector's response to unanticipated loads. For instance, the user may want different rates of compliance for flexion compared to that of extension. The prototype described here uses a 60 lbf/in die spring (McMaster-Carr # 9584K15) for each of the flexor and extensor tendons. Alternate setups are also possible with the spring guide to achieve a composite, non-linear spring stiffness. A non-linear response can be achieved by nesting a preloaded

spring and disc washer within the main spring. The interior spring would be held in place by disc washers held against the stepped features of the spring's guide shaft (Fig. 3c).

B. Key Features

Both flexion and extension are achieved with a single actuation unit, with one actuator per revolute joint. Tendon stiffness and pretension can vary depending on the assigned joint and desired response to unanticipated loads. The zero-backlash back drivable motor module simplifies the design along with reducing the size of the motor bank necessary to control all degrees of freedom of the end effector. Use of a one-way bearing in the pulley allows the motor module to be compact and robust. The desired preload maintained with the one-way bearing ensures that the wire wrapped pulley will not unspool even in the case of an unanticipated load or rapid rotation.

The custom uniaxial loads cells are designed specifically for tendon loads for robotic grasp applications. Load cells are attached to a spring guide with a 1/16" diameter spring pin. The large diameter cap of the spring guide shaft constrains the die spring against the guide plate, allowing the load cell to move as a unit under high tendon loads. When one tendon, say a flexor, is loaded, a net torque will develop at the joint, the flexor's die spring will compress, and the extensor's die spring will extend and take up the slack in the extensor tendon.

The ease of setup between various end effectors is a major advantage of the actuation system. Such a modular setup will enable experiments with different end effectors, each with unique proprioceptive and tactile sensing capabilities, and the testing of similar control policies on different plants.

Coupling between the actuation system and the robot hand is done by linking tendons via fishing-style swivel clips (100 lbf SPRO Power Swivels). Attachments are made with the system in slack and then each individual tendon is brought to a desired preload with the lead screw tendon tensioning mechanism.

C. Control Setup

The motor module allows for multiple control structures including position, velocity, force, and impedance (by varying the motor current). The Maxon EPOS2 24/5 Motor Controller has sampling rates for position control of 1 kHz and current control of 10 kHz. With a quad count encoder the motor position can theoretically be controlled with a resolution of 1/2000 counts per revolution (1.3 μm of tendon displacement). However, in practice, the position control resolution is on the order of 1/1000 counts per revolution and actual tendon displacements are not likely to be on the order of microns.

Depending on the context of the grasp or manipulation task, the control structure can be switched on the fly. For automated closure of the hand around a novel object, the motor module can be set to a compliance mode which uses limits on joint torques for safety, as in commercially-available prosthetic hands such as the Touch Bionics i-LIMB [15]. Furthermore, by controlling motor current one can implement impedance control for each digit [16].

Maxon EPOS2 24/5 controllers also have built-in position profile modes with limited variability. Position profile mode allows the user to set the minimum and maximum motor acceleration and uses a trapezoidal velocity profile. The motor controllers communicate through an internal CANOpen (Control Area Network) network between the individual controllers. The master controller on the CAN network is capable of being connected to the central computer by either USB or the more robust industrial standard of RS-232.

The central computer interfaces with the motors through the use of a Maxon command library in C++. There are multiple options for communication with Maxon devices, but C++ was selected as it the main language used for additional pieces of equipment, such as the Shadow Dexterous Robot Hand and multimodal BioTac tactile sensors (Syntouch, LLC) [17].

We can also measure compliance indirectly by comparing joint-based Hall-effect sensor measurements and motor position encoder measurements. Such comparative information can be used in the control loop or as a safety fault in case the actuation and hand system experiences tendon slip or creep.

D. Preliminary Dynamic Testing

The dynamic response of a single motor actuation system was tested with 500 g masses attached to each of the two output tendons. The actuation system was clamped to the edge of a workbench and the masses were allowed to hang freely over the edge of the workbench. The motor was controlled in position control mode to produce sinusoidal waves having an amplitude of 180° of rotation at the motor output shaft, which is equivalent to 1.3mm of tendon excursion. A tendon excursion of 1.3mm is approximately equal to 15° of rotation at a joint having a 10 mm diameter actuation pulley.

The sine wave was implemented for the following frequencies: 3.33 Hz, 4 Hz, 5 Hz, 6.67 Hz, 10 Hz, and 20 Hz. Due to sensor limitations in the current experimental setup, encoder position sampled at 100 Hz was subjected to a forward and reverse low pass filter that does not distort phase (MATLAB's "filtfilt" function) and then differentiated twice to enable comparisons between the acceleration of the motor output shaft and that of the 500 g mass hanging from the end of a single tendon. Acceleration of the 500 g mass was recorded at 150 Hz using a six degree-of-freedom inertial measurement unit (MEMSense IM05-0600C050T00).

III. Results

Initial dynamic characterization was conducted on a single actuation unit, specifically the dynamic response of the compound pulley reduction and tendon tensioning system. Due to limitations of the experimental setup, we can only reliably report on input and output magnitudes at this time (Fig. 4). At a frequency of 6.67 Hz, the gain of the compound pulley reduction and tendon tensioning system is

approximately one. At a frequency of 10 Hz, a decrease in system gain occurs until the gain drops severely around 20 Hz.

The actuation system was also used to directly actuate a single joint in the 18 degree-of-freedom Shadow Dexterous Robot Hand (Fig. 5). For initial testing, a single actuation unit was used to actuate the proximal interphalangeal (PIP) joint of the index finger directly. The distal interphalangeal (DIP) joint, coupled to the PIP joint, also moved under actuation.

The attachment of the Shadow Dexterous Robot Hand tendons and removal of tendon slack were simple due to the lead screw tendon preloading mechanism. Using position control mode, the actuation unit flexed and extended the index finger at both low (1 Hz) and high (4 Hz) frequencies (see video supplement). Flexion and extension were smooth and highly sensitive to small motor displacements. Figure 5 shows the rapid cycling of flexion and extension at a rate of 415 mm/min. The motion is shown in 0.25 sec increments. The wire rope "walked" smoothly along the pinion of the first stage of the pulley reduction without interfering with itself (see white arrows in Fig. 5).

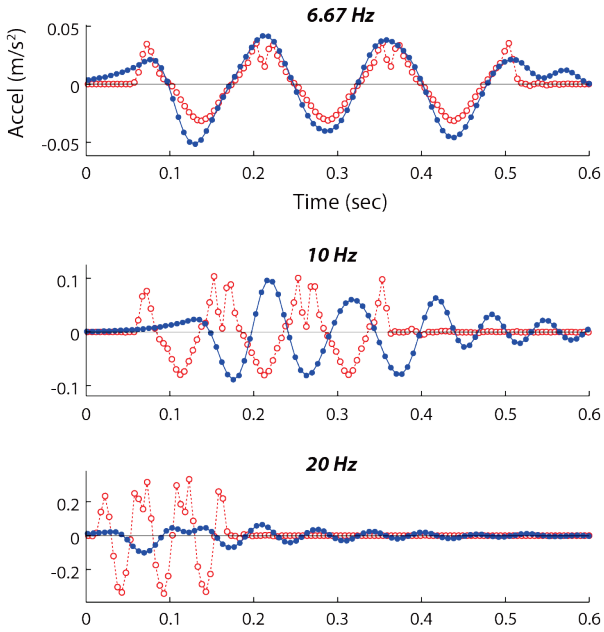

Fig. 4. Dynamic response of compound pulley reduction and tendon tensioning system. At a frequency of 6.67 Hz (top), the magnitude of the acceleration of the 500 g free-hanging mass (closed circles, solid line) is comparable to that of the motor shaft output (open circles, dotted line). Decreases in the system gain are shown for 10 Hz (middle) and 20 Hz (bottom). Phase shift is estimated for visualization purposes only.

IV. Discussion

A. Advantages of Design

The main advantages of the actuation system are its modularity and ease of setup and control of different tendon-driven mechanisms. A single actuation unit is capable of controlling both flexion and extension while maintaining a tendon preload and stiffness for unanticipated loading of a fingertip, for example. The compression springs, in particular, affords deformation in the overall system that provides safety from unexpected loading of the finger. Various springs with different spring constants can be installed on a joint-specific basis depending on desired behaviors. In the two tendon back-driveable configuration (N-type) each tendon can have user-defined tension preloads due to the modular compression spring while the motor output shaft is traveling to or maintaining a desired joint angle.

Attachment between a remote bank of actuation units and the robot hand will be made via a bundle of low friction tendon sheaths. This will allow for a flexible, kink-resistant, and low-friction attachment of tendons from the actuation system to the robot hand as the hand is moved in the workspace.

Actuation units can be mounted such that each additional unit's controller can be linked to the existing EPOS CAN network and assigned a node value directly on the controller. The EPOS2 24/5 CAN network has a maximum of 128 separate nodes which is more than sufficient for an anthropomorphic robot hand.

The Shadow Dexterous Robot Hand requires 18 modules for complete double-acting, N-type actuation. Two actuation units can be operated with only a single output tendon to accomplish co-contraction in a 2N-type actuation scheme. Individual joints on a robot hand can be manually changed between single-acting actuation and double-acting actuation depending on the control architecture. To reduce control complexity, multiple tendons can be actuated simultaneously in order to produce synergistic joint movements or control underactuated manipulators. Preliminary tests suggest that the actuation system will enable high frequency responses that can match or exceed those of the human hand. As such, the actuation system presented here is appropriate for a robotic hand testbed that is capable of producing fast, reflex-like grip responses.

B. Disadvantages of Design

Due to size and weight issues, the bank of actuation units cannot be located on the robot arm itself without severely limiting the payload of the robot hand. The motor bank will be placed alongside the base of the robotic arm and will require lengths of tendon sheathing to route tendons flexibly up to the robot hand. However, this is acceptable for our current purposes of creating a tendon-driven robot hand testbed as opposed to a body-worn neuroprosthesis, for example. Efforts will be made to reduce the length of the tendon sheaths as much as possible in order to minimize frictional losses between the remote actuation system and the end effector. Weight and power consumption are both issues that require further attention in the development of a compact and efficient motor control bank, although they are not immediate concerns for the present outlet-powered, workbench-mounted testbed design. Since the design of the robot hand testbed is intended for use as a research tool to advance the functional capabilities of highly dexterous robot hands, the power consumption of the motor units and supporting systems has not been considered as a significant design criterion.

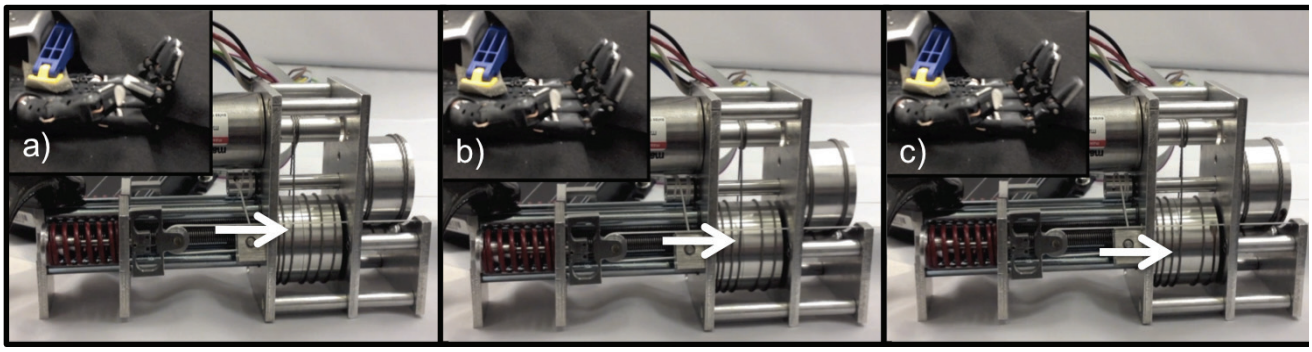

Fig. 5. Direct actuation of a single joint in the index finger of the Shadow Dexterous Robot Hand (inset). The *a*, *b*, and *c* snapshots show increments of 0.25 seconds (tendon rate of 415mm/min).

V. Future Work and Conclusion

An initial investigation of the dynamic response of the compound pulley reduction and tendon tensioning system has been conducted. However, additional work is needed to fully characterize the dynamic response, including how the natural frequency of the system is affected by different compression spring constants and/or tendon loads.

We have presented a novel design for a motor-based actuation system suitable for N-type or 2N-type control configurations for tendon-driven robotic hands. A working prototype has been constructed and further dynamic characterization of the actuation system is planned. A bank of these actuators will be used to drive the Shadow Dexterous Robot Hand as well as a custom anthropomorphic robotic hand that will be outfitted with multimodal BioTac tactile sensors [18] for grasp and manipulation experiments.

Acknowledgments

The authors would like to acknowledge Kevin Bair for his initial design of the actuation system and laying the foundation for the work presented. Leonard Bucholz and Andre Magdelano were instrumental in the machining and assembly of the actuation system and contributed to discussions of design concepts. James Kristoff assisted with interfacing the Maxon controllers with Linux using C/C++. Joshua Beck designed the strain-gage uniaxial load cell for tendon tension measurements.

References

[1] H. Liu, K. Wu, P. Meusel, N. Seitz, G. Hirzinger, M. Jin, Y. Liu, S. Fan, T. Lan, and Z. Chen, "Multisensory five-finger dexterous hand: The DLR/HIT hand II," in *Intelligent Robots and Systems, 2008. IROS 2008. IEEE/RSJ International Conference on*, 2008, pp. 3692–3697.

[2] R. Tubiana, "Architecture and functions of the hand," in *The Hand*, vol. 1, R. Tubiana, Ed. Philadelphia, PA: WB Saunders, 1981.

[3] A. M. Dollar and R. D. Howe, "The highly adaptive SDM Hand: Design and performance evaluation," *The International Journal of Robotics Research*, vol. 29, no. 5, pp. 585 -597, Apr. 2010.

[4] C. Loucks, V. Johnson, P. Boissiere, G. Starr, and J. Steele, "Modeling and control of the Stanford/JPL hand," in *1987 IEEE International Conference on Robotics and Automation. Proceedings*, 1987, vol. 4, pp. 573- 578.

[5] A. Nahvi, J. M. Hollerbach, Yangming Xu, and I. W. Hunter, "An investigation of the transmission system of a tendon driven robot hand," in *Proceedings of the IEEE/RSJ/GI International Conference on Intelligent Robots and Systems '94. "Advanced Robotic Systems and the Real World", IROS '94*, 1994, vol. 1, pp. 202-208 vol.1.

[6] F. Lotti, P. Tiezzi, G. Vassura, L. Biagiotti, G. Palli, and C. Melchiorri, "Development of UB Hand 3: Early results," in *Proceedings of the 2005 IEEE International Conference on Robotics and Automation, 2005. ICRA 2005*, 2005, pp. 4488- 4493.

[7] Shadow Robot Company, "Shadow Dexterous Hand." [Online]. Available: http://www.shadowrobot.com/hand/.

[8] C. S. Lovchik and M. A. Diftler, "The Robonaut hand: a dexterous robot hand for space," in *1999 IEEE International Conference on Robotics and Automation, 1999. Proceedings*, 1999, vol. 2, pp. 907-912 vol.2.

[9] T. E. Wiste, S. A. Dalley, T. J. Withrow, and M. Goldfarb, "Design of a multifunctional anthropomorphic prosthetic hand with extrinsic actuation," in *Proc of Intl Conf on Rehabilitation Robotics*, Kyoto, Japan, 2009, pp. 675-681.

[10] N. Gialias and Y. Matsuoka, "Muscle actuator design for the ACT Hand," in *Robotics and Automation, 2004. Proceedings. ICRA '04. 2004 IEEE International Conference on*, 2004, vol. 4, pp. 3380-3385 Vol.4.

[11] M. Grebenstein, M. Chalon, G. Hirzinger, and R. Siegwart, "Antagonistically driven finger design for the anthropomorphic DLR Hand Arm System," in *2010 10th IEEE-RAS International Conference on Humanoid Robots (Humanoids)*, 2010, pp. 609-616.

[12] S. Jacobsen, H. Ko, E. Iversen, and C. Davis, "Antagonistic control of a tendon driven manipulator," in *Robotics and Automation, 1989. Proceedings., 1989 IEEE International Conference on*, 1989, pp. 1334–1339.

[13] C. Melchiorri and M. Kaneko, "Robot hands," in *Springer Handbook of Robotics*, B. Siciliano and O. Khatib, Eds. Berlin Heidelberg: Springer-Verlag, 2008, pp. 345-360.

[14] F. Petit, M. Chalon, W. Friedl, M. Grebenstein, A. A. Schaffer, and G. Hirzinger, "Bidirectional antagonistic variable stiffness actuation: Analysis, design & Implementation," in *2010 IEEE International Conference on Robotics and Automation (ICRA)*, 2010, pp. 4189-4196.

[15] "Touch Bionics i-LIMB hand," [Online]. Available: http://www.touchbionics.com

[16] N. Hogan, "Impedance control - An approach to manipulation. I - Theory. II - Implementation. III - Applications," *ASME Transactions Journal of Dynamic Systems and Measurement Control B*, vol. 107, pp. 1-24, Mar. 1985.

[17] N. Wettels, A. R. Parnandi, Ji-Hyun Moon, G. E. Loeb, and G. S. Sukhatme, "Grip Control Using Biomimetic Tactile Sensing Systems," *Mechatronics, IEEE/ASME Transactions on*, vol. 14, no. 6, pp. 718-723, 2009.

[18] N. Wettels, V. J. Santos, R. S. Johansson, and G. E. Loeb, "Biomimetic Tactile Sensor Array," *Advanced Robotics*, vol. 22, pp. 829-849, Aug. 2008.